Bus Differential Protection Upgrade for a 1,500 MVA Nuclear Power Plant With Atypical Connections

Ronald Cole and Richard Tuck, *Dominion Energy,*
Thomas Solinsky, *Zachry Nuclear Engineering, Inc.,*
Carolyn Sun, Ritwik Chowdhury, Ahmed Abd-Elkader, and Bernard Matta,
Schweitzer Engineering Laboratories, Inc.

***Abstract*—A generator at a nuclear plant was being upgraded from 1,350 MVA to 1,500 MVA. The increase in rating required an upgrade to current transformers (CTs), which introduced mismatched ratings for the bus protection. The mismatched CT ratings favored the application of a digital bus differential relay.**

One set of CTs had atypical connections since they were a pair of three-phase CTs inside the delta winding of the generator step-up (GSU) transformer that consisted of three single-phase transformers. The plant also had a low-voltage generator circuit breaker (GCB). With the GCB open, high-voltage system ground faults could induce circulating currents in the GSU delta winding without any of the other zone CTs seeing any current. Unequal saturation of the CTs inside the delta winding could result in a possible unrestrained operation of the bus differential relay, thereby challenging protection security.

In this paper, we present the bus differential application and detail the associated hardware-in-the-loop (HIL) model, tests, and results. The results include examining security for external faults, verifying dependability for internal faults, and confirming a selective alarm for a CT failure condition.

I. Introduction

Bus differential protection (87B) uses the principle of Kirchhoff's current law to provide sensitive and fast bus protection. This paper discusses an application of a percentage-restrained bus differential relay for an upgraded 1,500 MVA generating unit at a nuclear power plant with external fault current levels exceeding 300 kA. The percentage-restrained differential relay was chosen because the upgrade required the installation of new current transformers (CTs) that mismatch the other CTs of the bus zone. An additional challenge for this application was the placement of six CTs inside the generator step-up transformer (GSU) delta winding that required secondary wiring compensation to allow application of the old electromechanical high-impedance bus differential relays. The new relay used the same CT and control circuits as the old relays as much as possible to simplify installation and reduce cost.

This paper discusses the testing performed to confirm proper behavior of the new 87B relay for this application. While the discussion is focused on the bus differential element, some of the concepts are also applicable to a generator differential element.

II. 1,500 MVA Nuclear Generator and Protection Upgrade

The generator in the nuclear power plant was upgraded from 1,350 MVA to 1,500 MVA. The associated rated output current would increase from 32.5 kA to 36.1 kA. This required an upgrade of the generator terminal CT ratio (CT1 in Fig. 1) from 35000:5 to 45000:5.

The GSU is comprised of three single-phase transformers, which is typical for large installations to aid transportation. The winding configuration was YNd11 (with a DAB connection). The GSU low-voltage (LV) delta winding connection was external to the transformers with CT2 inside the delta. The current inside the delta is $1/\sqrt{3}$ of the rated current during normal operation (i.e., an increase from 18.8 kA to 20.8 kA due to the higher generator rating). This increase in current was still within CT2 ratings; hence, they were not upgraded.

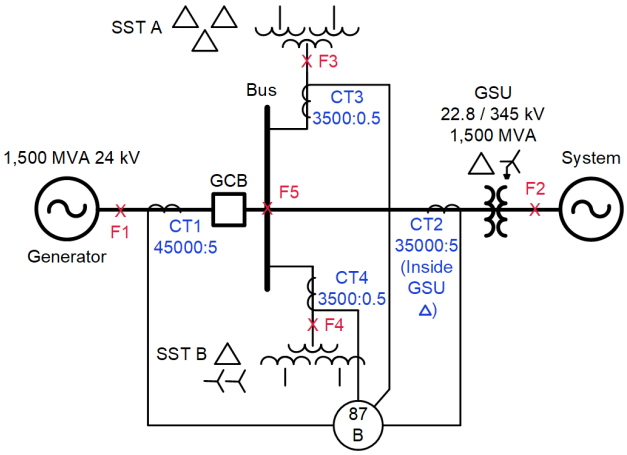

Fig. 1. Simplified single-line diagram of the nuclear power station.

The CTs connected to the station service transformers (CT3 and CT4) had a primary rating of 3,500 A due to their size. Their secondary rating was 0.5 A to match the existing CT ratios (35000:5) allowing the application of the original electromechanical 87B relays. One question we had to answer was whether applying relays with more sensitive current inputs (e.g., 1 A instead of 5 A nominal) to better match the 0.5 A CTs would improve sensitivity. The 5 A rated inputs turned out to be the better choice based on test results, as explained in Section V.

An additional consequence of the lower 0.5 A secondary nominal current rating of the CTs is cost savings due to lower copper requirements, but a lower rating can lead to higher CT winding resistance making CT performance more of an issue, which challenges differential protection. Security is a big concern for nuclear power plants. A misoperation would result in a forced outage with associated costs of millions of dollars in lost revenue, in addition to the adverse impacts on the electric grid and the need to compensate for the lost generation. Therefore, verifying the reliability of the system using hardware-in-the-loop (HIL) testing was important. The plant also had an LV generator circuit breaker (GCB), as shown in Fig. 1. This was an important application consideration and is discussed in Sections II and V.A.2.

A practice in this power plant to improve reliability was to wire three series pairs of 87B output contacts in parallel, as shown in Fig. 2, to trip the bus lockout relays. The reliability of the bus differential scheme is improved if one output contact has a mechanical or hardware failure and closes while the other contact in the series remains open. Dependability is improved due to the parallel connection paths.

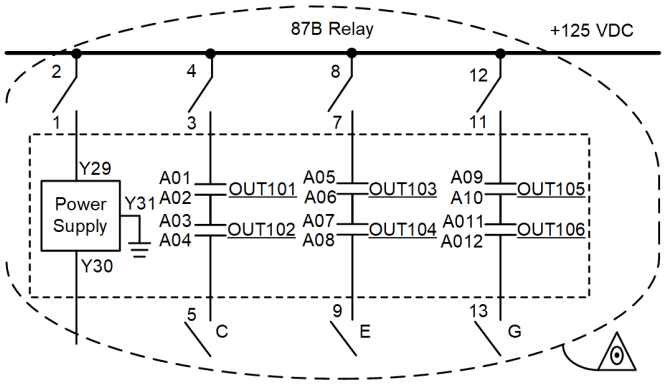

Fig. 2. Bus differential relay output configuration for lockout tripping.

Unlike most large generators in North America, the nuclear generator discussed in this paper was high-impedance grounded through a neutral reactor (instead of a resistor), often referred to as resonant grounding. Resonant grounding compensates for the generator zone capacitances (i.e., contributions from the stator winding insulation, iso-phase bus, and GSU) and reduces the ground fault current to near zero [1]. Due to the high-impedance grounding, the bus differential element was not expected to operate for single phase-to-ground (PG) faults. Hence, for the scope of this paper, the focus is only on phase-to-phase (PP) and three-phase (3P) faults at the generator voltage level. It is worth noting that these fault types are extremely rare in an iso-phase bus, but they can cause significant damage if they do occur.

III. System Model for HIL Testing

A. Generator Model

Modeling is often a balancing activity between:

- Available system parameters
- Complexity of the model and associated run-time
- Objective of the model and the tests to be performed

For this application, the objective was relay selection (5 A nominal versus a mix of 5 A and 1 A nominal inputs) and evaluation of the security and dependability of the 87B relay. The generator excitation and governor system parameters were not available. So, a simple voltage source behind a reactance model was deemed adequate for our application. Since the 87B relay was expected to operate within one cycle after a fault, the generator subtransient reactance was used as the source impedance. The generator was left ungrounded and any capacitances to ground were not modeled.

B. Fault Locations and Fault Types

The fault locations are shown in Fig. 1 and provide an adequate range of coverage for the tests.

- F1 was placed at the generator terminals to ensure 87B remains secure, the system remains selective, and the targeting is accurate for a stator winding fault.
- F2 was placed at the high-voltage (HV) terminals of the GSU, since we wanted to observe 87B behavior for the most common types of system faults. This fault location also challenges security of the 87B element since the CTs are inside the GSU delta.
- F3 and F4 were placed at the generator voltage level. These locations are the worst-case scenarios, since for a fault at F3, CT3 would measure the combined fault current contribution from the generator and the system.
- F5 was the internal bus fault location to test dependability.

The fault types considered were 3P and PP for locations at the generator voltage level, since zero-sequence currents for PG and double-phase-to-ground faults would be negligible. At F2, the 3P and PG faults were tested.

C. Atypical CT Connections and Resulting Behavior

As noted in Section II, CT2 was inside the GSU delta winding. Additionally, instead of there being three CTs (one for each phase), there were six CTs representing CT2. The six CTs were needed for the old electromechanical high-impedance 87B relay and are used for the new digital 87B relay to simplify installation and reduce cost. These CTs were wired such that no additional phase angle or magnitude compensation were needed for the bus differential scheme. The secondary relay currents were in-phase with the phase currents of the GSU delta winding flowing into the bus zone and scaled by the CT2 ratio.

The CT2 connections are shown in Fig. 3. Consider, for example, the primary A-phase current (I_{A2}) flowing into the bus zone. I_{A2} was equal to the difference in the delta-winding currents ($I_{A\Delta} - I_{B\Delta}$). Similarly, following the currents in the secondary winding, the secondary A-phase current provided to the relay (I_{a2}) is equal to the secondary delta-winding currents ($I_{a\Delta} - I_{b\Delta}$). Wire C01 was connected to the polarity of a relay current input, and I_{a2} is returned on Wire C12. No additional phase angle or magnitude compensation were needed for I_{a2}. The other primary phase currents into the bus zone were replicated for the relay in the same way.

The CT connections in Fig. 3 behaved similarly to delta-connected CTs with differences in burden (see Section III.D.1

and fault currents. The path of currents for a CA fault on the bus is shown in Fig. 4. For this fault, as with an AG fault on the HV side of the GSU, the CT connections are wired so that only the C-phase and A-phase differential elements see a fault current.

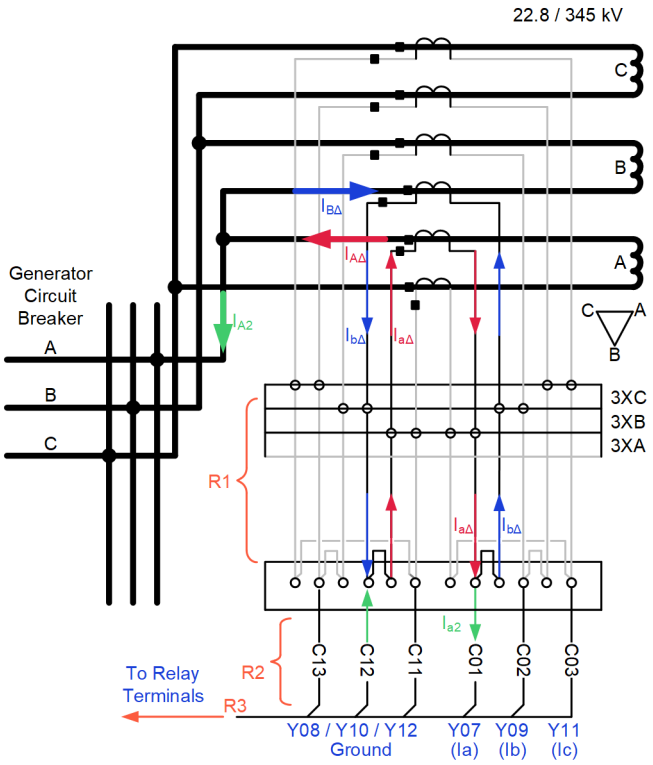

Fig. 3. CT secondary compensation for the GSU delta-winding currents.

A PG fault on the high-side of the GSU induces a circulating current inside the delta-winding. When the GCB is open, this circulating current becomes a pure zero-sequence quantity, and none of the other CTs see any current, as shown in Fig. 5. Due to the CT2 connections, the currents are expected to circulate between the two CTs, but unequal saturation of these CTs can result in an error operating current to the differential zone without any restraint provided by the other CTs. This scenario was an important application consideration and is explained in more detail in Section V.A.2.

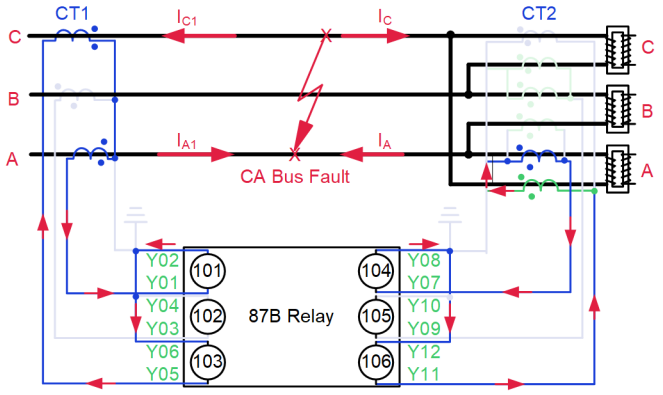

Fig. 4. Current flow for an internal CA fault or HV AG fault.

Since the CT secondary connections compensated for the CTs located inside the GSU delta winding, no compensation was required from the differential element. Therefore, the 87B relay was connected according to Fig. 6. Odd numbered terminals correspond to the polarity of the relay current inputs.

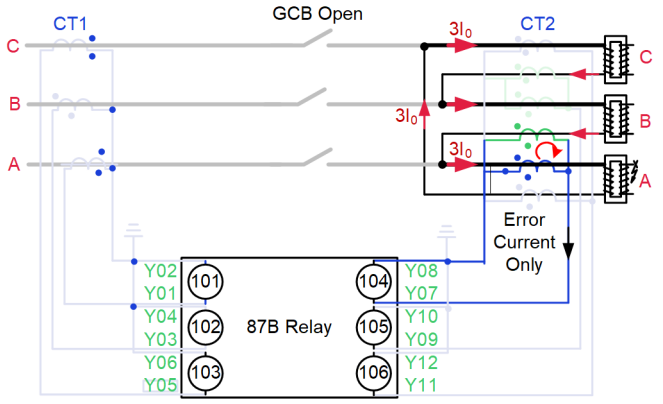

Fig. 5. Current flow for a HV AG fault with the GCB open.

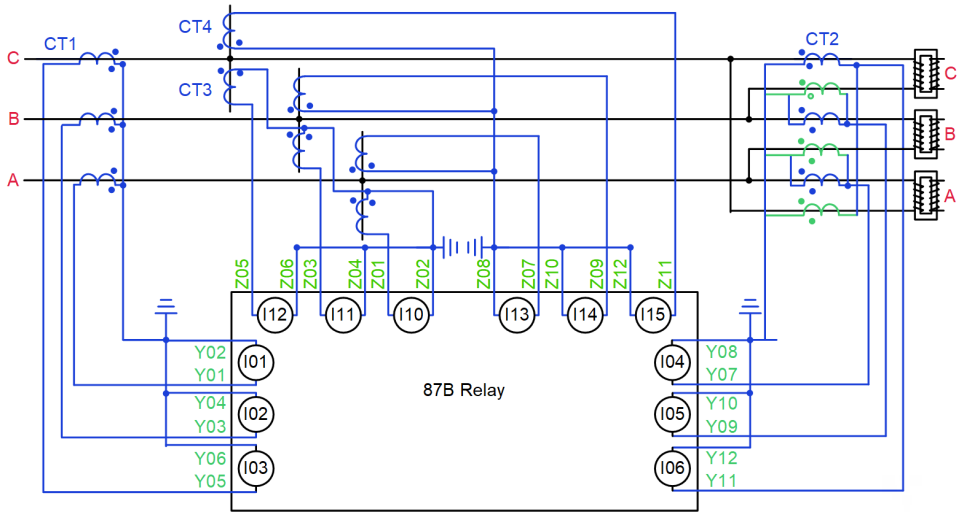

Fig. 6. CT connections to the bus differential relay.

D. CT Model for HIL Testing

CT models in Electromagnetic Transients (EMT) programs used for protection studies typically do not consider the secondary wiring of the CTs and are represented as per-phase components with the equivalent circuit instead, shown in Fig. 7. R_{CT} is the CT internal winding resistance, and R_B is the burden resistance. L_{CT} is the CT leakage inductance, negligible for a toroidal CT with uniformly distributed secondary windings. L_B is the burden inductance, neglected because digital relays do not have the same large inductive burden as electromechanical relays.

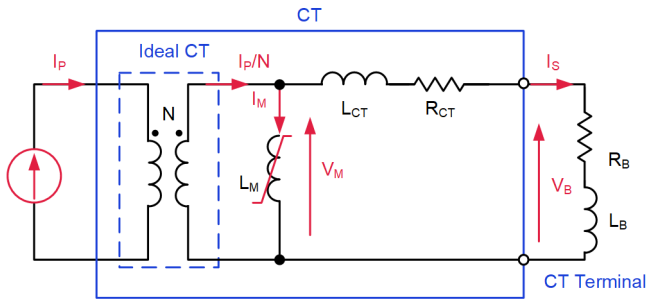

Fig. 7. CT equivalent circuit model, typically used for protection studies.

1) Burden Calculations

To accurately translate the physical system data to the CT model parameters, we had to consider the behavior of the CTs for the different fault types and captured the equivalent CT burden resistance. It was important to do this accurately to be confident in our conclusions regarding security for this critical application. The CT lead lengths shown in Table I were provided by the plant. The associated Resistances R1, R2, and R3, shown in Fig. 3, were calculated based on cable data and are explained as follows:

- R1 connects the CT to the panel that provides the delta connection. This resistance only applies to CT2.
- R2 connects the panel to an intermediate connection box for CT2. For the other CTs, it connects the CT to an intermediate connection box. These are existing cable runs reused for the new relay.
- R3 connects the intermediate connection box to the relay.

TABLE I
CT LEAD LENGTHS AND RESISTANCES

CT	Lead Length (Feet)	Lead Width (American Wire Gauge)	Lead Resistance (Ω)
CT1	R2: 45 R3: 700	12 8	R2: 0.0997 R3: 0.6125
CT2	R1: 162 R2: 370 R3: 830	10 10 8	R1: 0.2009 R2: 0.4588 R3: 0.7263
CT3	R2: 880 R3: 185	8 8	R2: 0.7700 R3: 0.1619
CT4	R2: 777 R3: 191	8 8	R2: 0.6799 R3: 0.1671

An example burden calculation for CT2 can be calculated based on the current relationships shown in Fig. 3. The burden voltage (V_B) for the A-phase CT may be calculated using (1).

$$V_B = I_A \bullet R1 + (I_A - I_B) \bullet (R2 + R3) \quad (1)$$

Applying (1) for the different fault types, the burden resistances for the CT2 model are as follows:

- For a PP fault on the GSU LV side, as shown in Fig. 8, the fault current splits between one transformer in parallel with two transformers. This causes the current on the A-phase CT2 pair to be twice as large and opposite in polarity as on the B- and C-phase CT2 pairs. Thus, for a PP fault, substituting I_B with $-0.5 \bullet I_A$, the burden voltage ($V_{B\text{-}PP}$) may be expressed as a function of the secondary fault current ($I_{FLT\text{-}PP}$) and lead resistances as shown in (2). The burden resistance ($R_{B\text{-}PP}$) is obtained by dividing both sides of (2) by the current and may be expressed using (3).

$$V_{B-PP} = I_{FLT-PP} \bullet (R1 + 1.5 \bullet (R2 + R3)) \quad (2)$$

$$R_{B-PP} = R1 + 1.5 \bullet (R2 + R3) \quad (3)$$

The behavior for a GSU HV PG fault with the GCB closed is similar and the burden of (3) is conservative and can be applied.

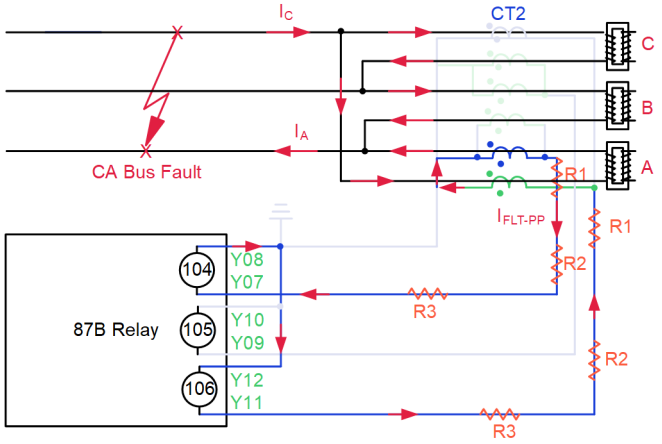

Fig. 8. Current flow for a LV CA fault or HV AG fault.

- For 3P faults, I_B is substituted in (1) with $I_A \angle -120$ degrees. This gives a CT2 3P fault burden voltage represented by (4), (5), and (6) with a corresponding burden resistance shown in (7).

$$V_{B-3P} = I_A \bullet R1 + (I_A - I_A \angle -120°) \bullet (R2 + R3) \quad (4)$$

$$V_{B-3P} = I_A \bullet R1 + \sqrt{3} \bullet (I_A \angle 30°) \bullet (R2 + R3) \quad (5)$$

$$V_{B-3P} = I_A \bullet (R1 + \sqrt{3} \angle 30° \bullet (R2 + R3)) \quad (6)$$

$$R_{B-PP} = R1 + \sqrt{3} \angle 30° \bullet (R2 + R3) \quad (7)$$

The burden voltage for the 3P fault is unique since it is shifted in phase relative to the secondary current due to the dependency on current from another phase. The CT model of Fig. 7 does not accommodate this scenario

well due to the lack of coupling between the phases. For our application, we assumed the worst case by ignoring the 30-degree phase shift, which results in a higher calculated burden resistance.

- For PG faults at Location F2 with the GCB open, the burden impedance is simply twice of R1. This is a slightly conservative estimate since any error current due to CT saturation flowing through R2 and R3 lowers the CT burden and saturation voltages, which in turn reduces the error current.

The CT burden resistances for the different fault types considered are summarized in Table II.

TABLE II
CT BURDEN RESISTANCES FOR DIFFERENT FAULT TYPES

CT	PP Fault (Ω)	3P Fault (Ω)	PG Fault at F2 with GCB Open (Ω)
CT1	0.7122	0.7122	N/A
CT2	1.9785	2.2535	0.4018
CT3	0.9319	0.9319	N/A
CT4	0.8470	0.8470	N/A

2) CT Ratio, Resistance, and Excitation Curve Data

The CT model parameters such as CT winding resistance (R_{CT}), knee-point voltage (V_{KNEE}), and saturation voltage (V_{SAT}) are shown in Table III. These parameters were available for the existing CT2, CT3, and CT4 but were not available for the new CT1 since the replacement had not been purchased.

For R_{CT} of CT1, we used the same ohms-per-turn ratio as CT2 (0.686 mΩ per turn) to obtain the value shown in Table III. The ohms-per-turn ratio for a CT with such high primary-rated currents can be quite small due to the size of wires used. A 2.5 mΩ-per-turn value has been used as a typical value in the past, that value is only valid for lower ratio 5 A nominal CTs [2]. CT3 and CT4 had a high ratio but had a lower (0.5 A) nominal rating; hence, they had a resistance of 3.61 mΩ per turn.

For the excitation characteristics, the plant specified that the replacement for CT1 would be a C800 CT and to use the standard C57.13 curves [2]. So, the C57.13 curve was extrapolated for a 1200:5 CT using the estimated CT resistance to obtain the CT1 characteristics shown in Fig. 9. The rest of the CTs had detailed available data. For the model, we used 10 current and voltage pairs to represent the excitation characteristics of the CT. The approximate V_{KNEE} and V_{SAT} are summarized in Table III.

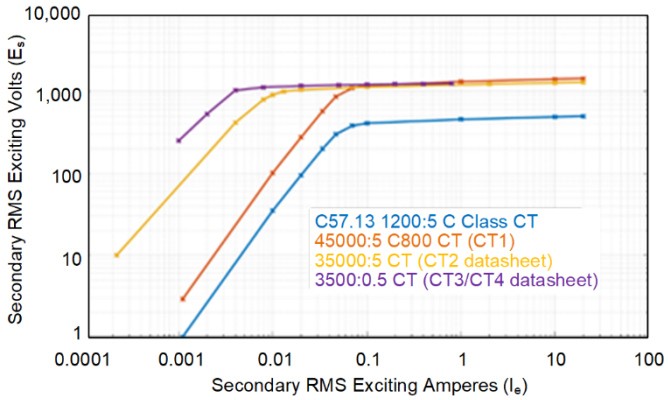

Fig. 9. CT excitation characteristics.

TABLE III
CT MODEL PARAMETERS

CT	CTR	R_{CT} (Ω)	V_{KNEE} (V)	V_{SAT} (V)
CT1	45000/5	6.17	900	1,400
CT2	35000/5	4.80	900	1,300
CT3	3500/0.5	25.25	1,000	1,300
CT4	3500/0.5	25.25	1,000	1,300

3) Remanence

The maximum level of remanence that may be expected in a CT is often available in CT test reports. The remanence level is not typically provided in the CT data sheet, and this parameter was not available to us. IEEE and IEC guides provide surveys on the level of remanence found in CTs installed in the field and were consulted [3] through [5]. The maximum levels were typically in the vicinity of 80 percent.

An estimate of the remanence level to consider for fast protection elements (those with subcycle operation) can be made based on the ratio of V_{KNEE} to V_{SAT} [5]. This is because the losses increase as the CT operates above its knee region and load current brings the remanence level back to the CT's linear operating region. For our CTs shown in Table III, the maximum ratio of V_{KNEE} to V_{SAT} was around 75 percent, which is what we used. To minimize the number of permutations of cases to be run, we used the following three scenarios:

1. $CT1_{REM}$ = 0%, $CT2_{REM}$ = 0%, $CT3/4_{REM}$ = 0%
2. $CT1_{REM}$ = 75%, $CT2_{REM}$ = –75%, $CT3/4_{REM}$ = 75%
3. $CT1_{REM}$ = 0%, $CT2_{REM}$ = 75%, $CT3/4_{REM}$ = 0%

When testing with the different point-on-waves of fault inception, these permutations were considered to be a more-than-adequate representation of the different scenarios the system would encounter in its lifetime.

E. Model Verification

1) Primary System EMT Model Verification

The plant model was developed in a short-circuit program (SCP). For HIL testing, the system had to be modeled in a real-time digital simulator (RTDS). The RTDS model fault currents were compared with those from the SCP model to verify model accuracy. The comparison is shown in Table IV, and the errors were insignificant, confirming that the RTDS model closely matched the SCP system model. Typically, a similar comparison is done for PG faults, but since this was a resonant grounded system, the performance was compared for PP faults that yielded similar accuracy (not shown).

TABLE IV
RTDS VERSUS SCP FAULT CURRENTS (FOR A 3P FAULT)

Fault Location	Current Terminal	SCP (kA)	RTDS (kA)	Error (%)
F1	CT1	207.6	207.40	–0.10
F2	CT2	76.52	77.25	+0.95
F3	CT3	308.7	307.00	–0.55
F4	CT4	308.7	307.00	–0.55
F5	CT1	102.6	102.70	+0.10
	CT2	209.9	207.50	–1.16

2) CT Model Performance Verification

The time-to-saturate is a reasonable indication of CT model accuracy and depends on the CT saturation factor (K_S), which depends on the application parameters [3] [5]. K_S can be calculated using the worst-case external fault current (I_S) along with the other CT known parameters using (8).

$$K_S = \frac{V_{SAT}}{I_S \bullet (R_{CT} + R_B)} \tag{8}$$

For the example CT3, the K_S equals 1.126 after calculating (9).

$$K_S = \frac{1300\ \text{V}}{\left(\frac{308.7\text{E}3}{7000}\right) \bullet (25.25 + 0.9319)} = 1.126 \tag{9}$$

A fully offset per-unit fault current waveform (10) was used to verify the expected time-to-saturate. Since it is in a generating plant, the X/R ratio for this system was very large. Large X/R ratios have little impact when considering time-to-saturate [5], so a value of 100 was used. See (11), (12), and (13).

$$I_{\text{fully-offset}} = \sin(\omega t + \theta) - \sin(\theta) \bullet e^{-\left(\frac{t}{\tau}\right)} \tag{10}$$

$$\theta = -\tan^{-1}\left(\frac{X}{R}\right) = -89.43° \tag{11}$$

$$\tau = \frac{1}{\omega} \bullet \left(\frac{X}{R}\right) = 0.2653\ \text{s} \tag{12}$$

$$\omega = 2\pi f_{sys} = 377\ \text{rad/s} \tag{13}$$

Equations (9) and (10) can be applied to find the intersection point and the associated time-to-saturate. This is represented by Fig. 10 showing a time-to-saturate of 4.5 ms. The RTDS CT model response is shown in Fig. 11 and has a time-to-saturate of 4.75 ms, which is reasonably accurate.

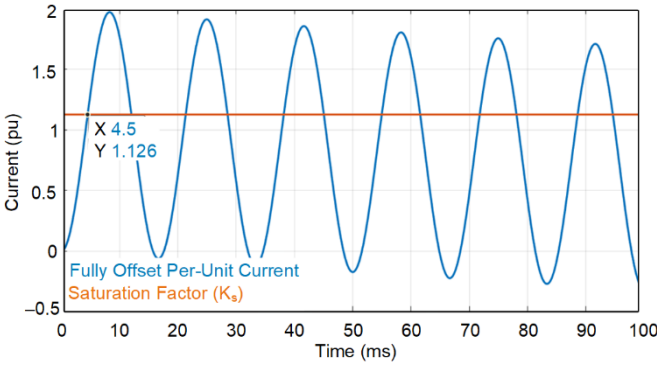

Fig. 10. Time-to-saturate for a fully offset waveform for the application specific saturation factor.

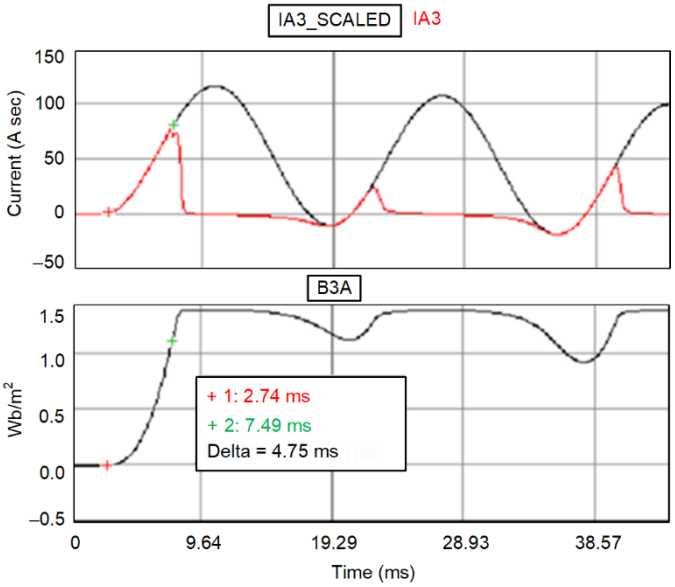

Fig. 11. Performance of RTDS CT model.

Fig. 11 also shows the flux density of the different CTs. With remanence, it may have a higher or lower initial value, making the CT saturate earlier or later, respectively.

IV. DIFFERENTIAL ELEMENT AND SETTINGS

One of the objectives for HIL testing was the selection of an appropriate relay. This section gives an overview of the relay settings that were selected for this application based on the test results of Section V.

A. Differential Element Overview

The digital bus differential relay selected for this application has an adaptive algorithm described in Fig. 12 [6]. If an external fault is detected with a possibility of resulting CT saturation, CON*n* (where *n* = 1, 2, 3 etc.) asserts, and the relay uses the secure Slope 2 (SLP2) setting; otherwise, the relay would continue to use the sensitive Slope 1 (SLP1) setting to be able to declare an internal fault using the restrained differential bit

(87R*n*). The external fault detector is described in Fig. 13; the element declares an external fault if there is an increase in restraint current (I_{RT}), while there is no corresponding increase in operate current (I_{OP}). An adaptive scheme offers numerous advantages relative to a fixed dual-slope characteristic, as discussed in [5].

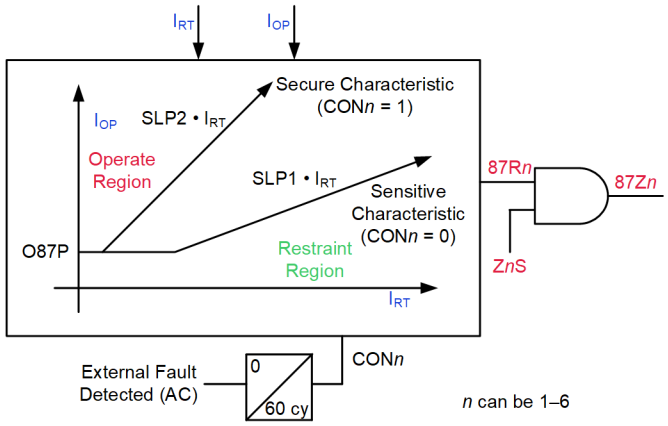

Fig. 12. Simplified bus differential relay algorithm.

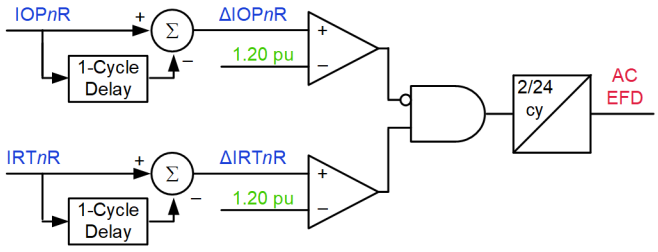

Fig. 13. External fault detector (alternating current [ac]).

The differential zone trip (87Z*n*) is also supervised by the Z*n*S setting, which, in our case, was used to block the differential element for a CT failure condition, as described in Section IV.C.

B. Differential Element Settings

The main settings from Fig. 12 that required consideration were the pickup (O87P), SLP1, and SLP2.

In this application, a O87P of 0.50 pu was used. This is sufficient to accommodate any steady-state CT errors. As we will see in Section V.A.2., the setting also provides adequate security for a power system ground fault (Location F2 in Fig. 1) with the GCB open.

The applied relay derives its I_{OP} using a phasor summation of the zone currents, and it derives its I_{RT} by summing the magnitudes of the zone boundary currents. SLP1 was set to 15 percent to accommodate steady-state errors, and SLP2 was left at a default, secure value of 80 percent.

C. CT Failure Detection

A CT failure can occur due to an open or a shorted CT. Various mechanisms for CT failure detection have been applied in the industry. Some approaches use the voltages wired to the relay; others use a mechanism to detect a step change in individual current inputs.

For our application, we used the built-in algorithm of Fig. 14, which declares a CT failure if the following conditions are true:

- There is a sudden increase in operate current (> 0.05 pu).
- There is a sudden decrease in restraint current (< 0.05 pu).
- The increase in the operate current and the decrease in the restraint current corresponded to each other (i.e., their sum is less than 0.05 pu). This condition may not be true if a CT failure occurs during CT saturation, but those scenarios are uncommon, since they involve multiple rare scenarios at the same time. Moreover, this condition added required security, as will be discussed in Section V.B.2.
- The operate current is larger than a sensitive pickup (S87P) of 0.10 pu.

The logic automatically resets if the operate current is small (less than 0.05 pu).

The Z*n*S settings supervising an 87Z*n* trip (shown in Fig. 12) were then set to "NOT OCTZ*n*" to allow the differential element to operate only when there is no CT failure.

Digital relays often provide a normally closed alarm output contact that may be used to notify an operator when the relay is out-of-service or has a malfunction detected by its self-diagnostic features. The CT failure (OCTZ*n*) indication was added to an alarm output contact.

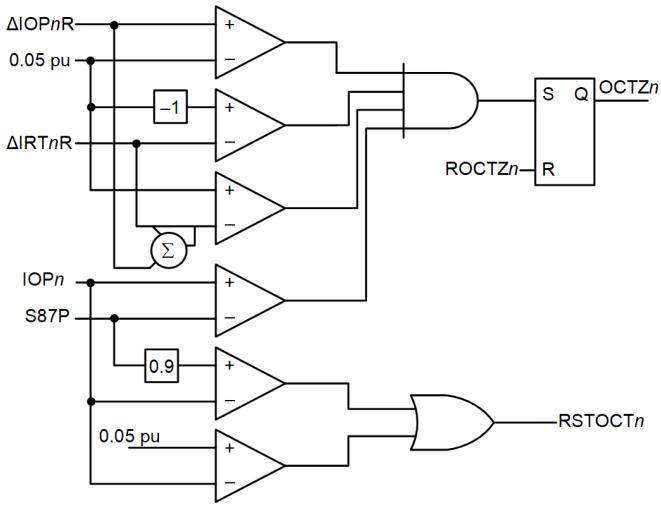

Fig. 14. CT failure detection logic.

V. Test Results

A. Security

1) Generator Online (GCB Closed)

The most common fault that the CTs in the power plant are likely to see are system ground faults (F2 in Fig. 1). The relay remained secure for this fault, as evident in Fig. 15. We can see some level of direct current (dc) saturation on CT1A current terminal 4 cycles into the event when IOP1 rises to 0.38 pu with an IRT1 of 1.91 pu, but the relay remains secure during this increase.

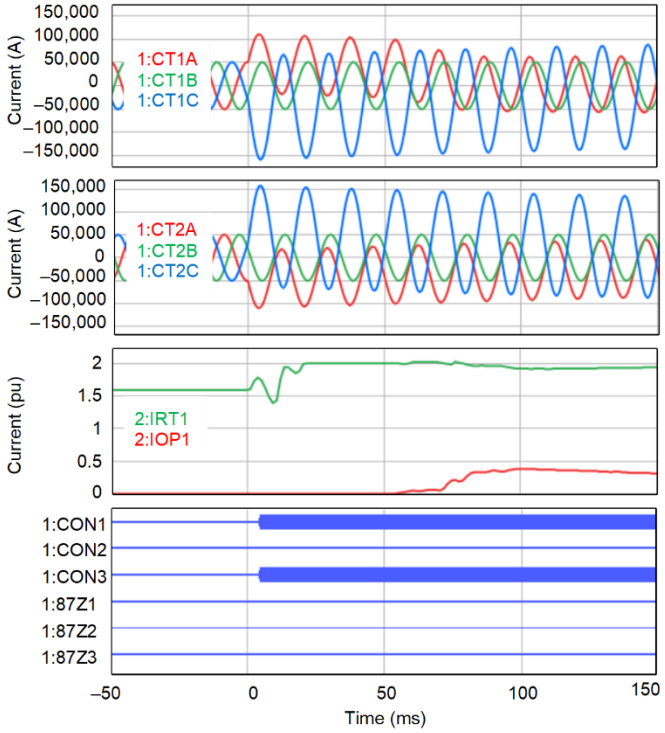

Fig. 15. Relay response to an external AG fault on the power system (F2).

A challenging security case was for a fault at F3/F4 when both the power system and the generator contribute to the fault current greater than 300 kA. Since CT3 and CT4 had the same R_{CT} but CT3 had a higher R_B, we placed a bolted fault at F3. The relay response is shown in Fig. 16 The relay remained secure for this condition despite severe saturation. The A-phase CT saturated first in 2 milliseconds since the fault occurred near a voltage peak (with no current dc offset), which resulted in a sharp increase in the current (i.e., the derivative of the current was highest) making it saturate first.

Having run the cases through a relay with configurable 1 A inputs in parallel, we noticed the analog-to-digital (A/D) converter saturate (or clip) the current waveform. For faults at this location, the currents could be greater than 300 kA, which corresponds to 850 kA peak after considering the dc offset. Considering the CT ratio of 7000, this corresponds to 120 A peak. While the 5 A nominal relay could reproduce a waveform accurately up to 250 A peak, the 1 A nominal relay could only do so up to 50 A peak. This did not impact security since the external fault detector of Fig. 13 was fast enough, but it did result in a misrepresentation of the primary currents that were in addition to CT saturation.

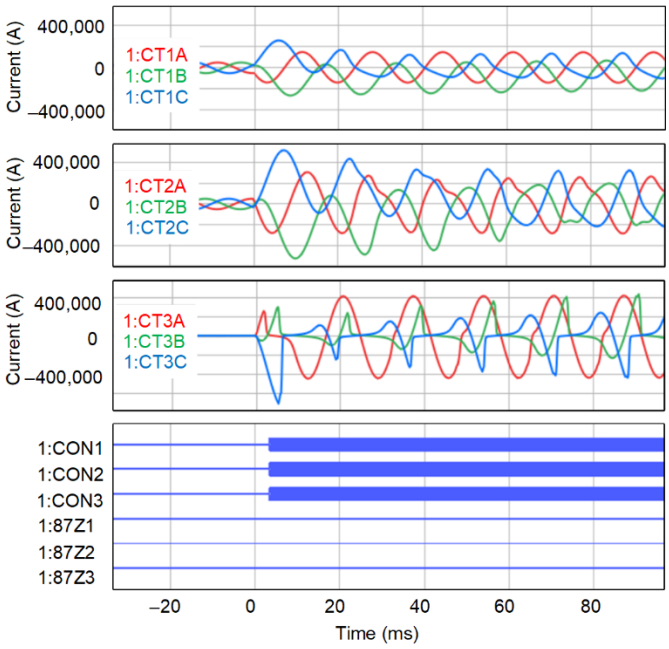

Fig. 16. Relay response to an external three-phase fault at Location F3.

2) Generator Offline (GCB Open)

An important security consideration for this application is the scenario of a system ground fault (F2 in Fig. 1) with the GCB open. In this scenario, there is a circulating current in the GSU delta winding and, if the CTs perform well or saturate equally, there are no currents to the relay at any of the terminals. Both I_{OP} and I_{RT} currents are zero. However, if the CTs saturate unequally, then the relay sees currents from CT2 and not the other CTs since the GCB is open, which makes I_{OP} and I_{RT} equal but non-zero. In such instances, if I_{OP} exceeds the pickup setting (O87P) of 0.50 pu, the differential relay will misoperate.

For a PG fault at F2, the ground fault current contribution on the HV side from the GSU on each of the three phases was 4.41 kA and equal in magnitude and phase. This current corresponded to a delta-winding circulating current of 38.5 kA primary and could be calculated using (14) and (15).

$$I_D = I_{flt} \bullet \left(\frac{V_{HV}}{\sqrt{3} \bullet V_{LV}} \right) \tag{14}$$

$$I_D = 4.41\ \text{kA} \bullet \left(\frac{345\ \text{kV}}{\sqrt{3} \bullet 22.8\ \text{kV}} \right) = 38.5\ \text{kA} \tag{15}$$

Since the circulating current in the delta is measured equally for all six CTs comprising CT2, and they all have practically the same CT winding and burden resistances (within 10 feet of secondary cable length differences), the only way for them to saturate unequally is to introduce mismatched initial remanence values to maximize the erroneous I_{OP} to the relay. A realistic level of remanence mismatch between the individual phase CTs was not clear to the authors and not covered in the literature. A worst-case remanence mismatch of 0.75 pu, 0 pu, and –0.75 pu on the A-, B-, and C-phases was used. Such a large level of

mismatch in remanence could occur if the system has a history of external faults with the GCB closed.

The behavior for a ground fault at F2 is shown in Fig. 17 for the large remanence mismatch. The relays only saw the error current from CT2, but the I_{AD}, I_{BD}, and I_{CD} currents from the delta winding from the RTDS are shown as reference. I_{OP}, in this case, reached a maximum value of 0.11 pu, which allowed the differential element to remain secure. It is also worth noting that the worst case is a fully offset current waveform since the saturation is slow, unlike the fault shown in Fig. 16, when the worst-case behavior occurred due to fast saturation from a no-offset fault current waveform.

This scenario was a critical consideration for this application. The external fault detectors (CON*n* bits) did not pickup, and the slopes associated with the differential element were not helpful since there was only one error current presented to the relay.

While this case did not challenge our application, a similar application (i.e., with GSU LV CTs inside the delta winding) in a smaller generating plant could face this issue. The issue is likely to be worse in a smaller generating plant with a lower transformer leakage impedance in relation to the system impedances, higher fault currents, higher burden resistance, and poorly sized CTs. While we had six CTs in the delta winding, the same issue would present itself in applications with three delta-connected CTs.

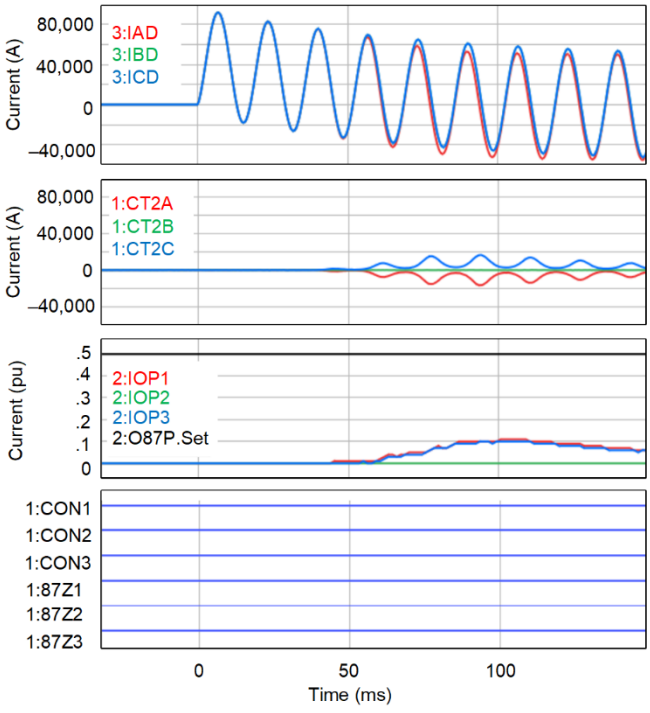

Fig. 17. Relay response to an AG fault at Location F2 with GCB open.

B. Dependability

The speed and sensitivity provided by the 87B relay were checked. One of the advantages of having an LV GCB is that a trip of the 87B zone breakers clears the fault. This contrasts with plants without an LV GCB, where the generator continues to feed a bus or a transformer fault despite a trip.

1) Speed

The relay generally operated for internal faults in less than 10 ms; an example of a 9-millisecond trip is shown in Fig. 18. This is one of the advantages of an adaptive characteristic compared to a dual-slope characteristic; a low-set SLP1 allows the adaptive differential element to operate quickly for heavy internal faults.

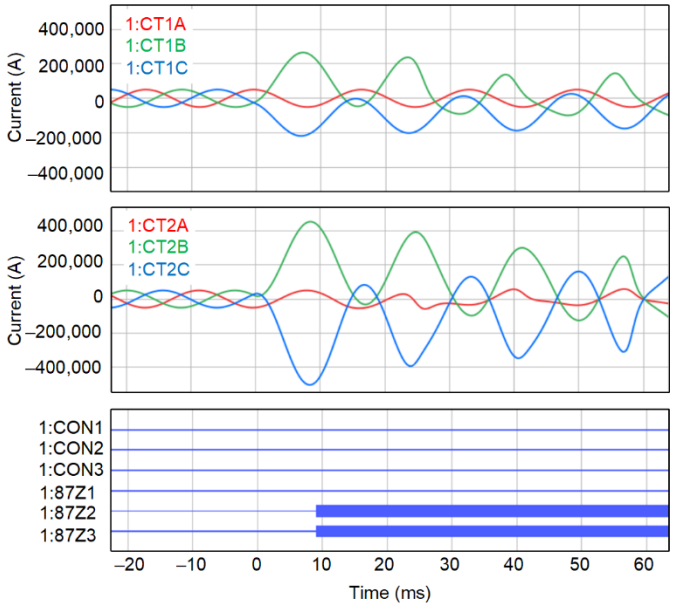

Fig. 18. Relay speed for a bolted internal BC fault at Location F5.

2) Sensitivity

Phase faults can have some arc resistance, as observed from field events [7] [8]. The fault resistance coverage provided by the differential element was approximately 1 Ω. While this may appear to be little fault resistance coverage, it is electrically a large resistance for this 24 kV, 1,500 MVA power plant that is normally surrounded by very small impedances from the generator and the power system. For reference, the generator base impedance was 0.384 Ω, and the subtransient reactance was 0.131 Ω, which was an eighth of the fault resistance. When including the system fault current contribution, this resulted in a large voltage drop, even across a small fault resistance; in turn, this resulted in a low fault current relative to the load current.

A 1 Ω BC fault is shown in Fig. 19. The phase current from the generator increased slightly, whereas the phase current from the system decreased. Overall, the restraint currents on both the B- and C-phases decreased. The operate current increased past 0.50 pu, which resulted in a trip.

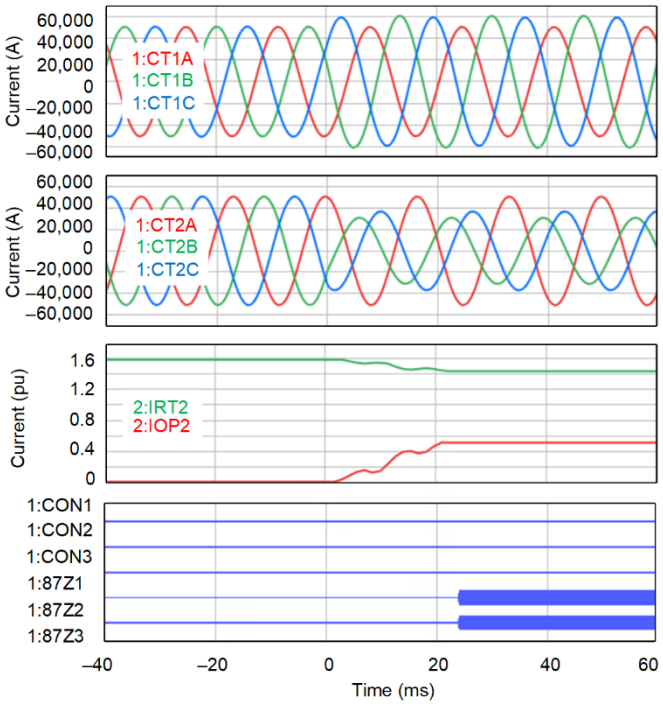

Fig. 19. Relay sensitivity for a 1 Ω internal BC fault at Location F5.

One may wonder why CT failure logic did not operate since there was an increase in operate and a decrease in restraint current. This is because of the additional security in the CT failure logic (Section IV.C) that verifies that the decrease in restraint corresponds to the increase in operate current, which was not true for this fault.

The internal fault current contribution from the station service transformers was negligible, so using a 1 A or 5 A relay did not make a difference in sensitivity.

Unlike some of the other performance metrics of a differential relay, the fault resistance coverage can be evaluated using a short-circuit program by considering the fault current contributions from the generator and the power system for a resistive fault in relation to the load currents.

C. *CT Failure Alarm*

As noted in Section II, a relay misoperation is very expensive, regardless of whether it is due to an external fault or a CT failure. More recently, the nuclear generation industry has shown increased interest in CT failure detection.

A CT1 failure on the A-phase is shown in Fig. 20. Even though 87R1 asserts, OCTZ1 prevents 87Z1 (A-phase differential zone) from tripping the unit. Instead, the normally closed alarm output contact (OUT108) deasserts. The reset mechanism for CT failure detection was also tested.

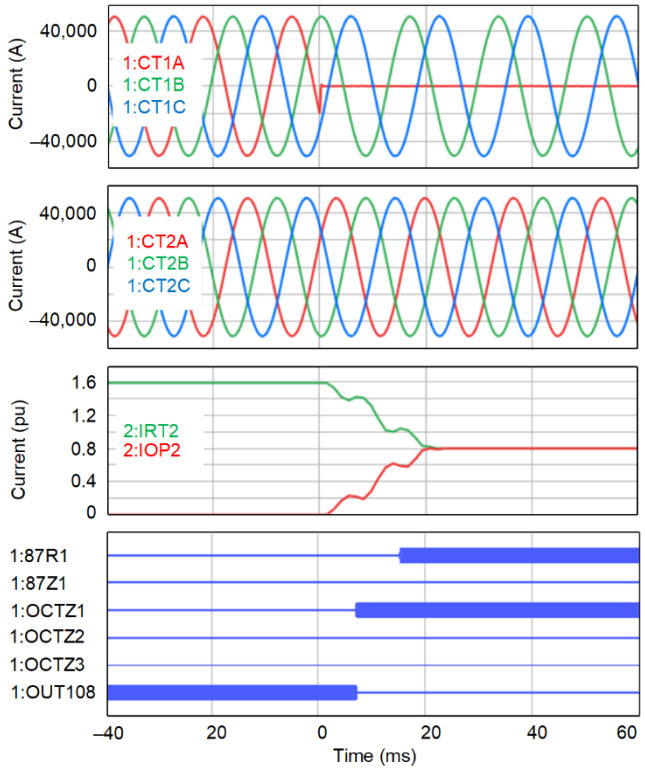

Fig. 20. CT failure detected by the relay.

D. *Summary*

The performance of the 87B relay is summarized as follows:

- The 87B relay remained secure despite heavy CT saturation in 2 milliseconds due to fault currents in excess of 300 kA.
- The 87B relay remained secure for HV PG faults with the LV GCB open and the CTs inside the GSU delta having large remanence mismatch.
- The relay typically operated in less than 10 milliseconds for bolted internal faults.
- The relay was set with a pickup of 0.50 pu and could see 1 Ω of phase fault resistance. While this may appear to be a small value, it is relatively large for a 24 kV 1,500 MVA power plant.
- CT failure detection worked reliably for this application, provided an alarm, and secured the 87B element from misoperating. This is an important security feature for any differential relay and can prevent a forced outage resulting in millions of dollars of lost revenue.
- A 5 A relay behaved better than a relay with mixed 5 A and 1 A inputs, since it provided a wider measurement range during an external fault. On the other hand, there was no loss of dependability in using the 5 A inputs, since the station service transformers contributed negligible fault current.

VII. Conclusion

This paper describes a bus differential application where a nuclear generator is being upgraded from 1,350 MVA to 1,500 MVA. This increase in rating resulted in upgrades to CTs, which introduced mismatched ratings for the bus protection scheme.

The GSU CTs were comprised of a pair of three-phase CTs inside the delta winding and were compensated for in the secondary wiring. This was a rare, atypical connection, and required careful analysis to model. Additionally, a ground fault on the HV system would induce circulating currents in the GSU delta winding. With the LV GCB open, this would result in a pure zero-sequence circulating current seen by the CTs inside the delta while the other differential-zone CTs do not see any current. Unequal saturation of the delta-winding CTs could result in a false, unrestrained misoperation of the differential element.

To verify the reliability of this critical nuclear application, HIL testing was performed. The test results showed security of the bus differential protection for external faults, despite heavy CT saturation. This security was achieved due to the low CT requirements of the bus differential relay. The relay also remained secure for unequal CT saturation from the circulating delta-winding currents despite large remanence mismatch. Dependability, both speed and sensitivity, was quantified and considered adequate for the application. The bus differential relay was also selective in detecting a CT failure condition, which allowed securing the differential element and alarming. A CT failure alarm can facilitate a planned plant shutdown, saving millions of dollars in cost.

VIII. Acknowledgements

The authors would like to thank Jason Young and Michael Thompson for sharing their expertise for this paper.

IX. References

[1] IEEE Standard C62.92.2-2017, *IEEE Guide for the Application of Neutral Grounding in Electrical Utility Systems, Part II – Synchronous Generator Systems.*

[2] IEEE Standard C57.13-2016, *IEEE Standard Requirements for Instrument Transformers.*

[3] IEEE C37.110-2007, *IEEE Guide for the Application of Current Transformers Used for Protective Relaying Purposes.*

[4] IEC TR 61869-100:2017, *Guidance for Application of Current Transformers in Power System Protection.*

[5] R. Chowdhury, D. Finney, N. Fischer, and D. Taylor, "Determining CT Requirements for Generator and Transformer Protective Relays," proceedings of the 46th Annual Western Protective Relay Conference, Spokane, WA, October 2019.

[6] *SEL-487B-1 Bus Differential and Breaker Failure Relay Instruction Manual*. Available: selinc.com.

[7] D. Miller, "Three Phase Bus Fault with Fault Impedance," proceedings of the 42nd Western Protective Relaying Conference, Spokane, WA, October 2015.

[8] C. Henville and R. Chowdhury, "Coordination of Resistive Reach of Phase and Ground Distance Elements," proceedings of the 48th Western Protective Relaying Conference, Spokane, WA, October 2021.

X. Biographies

Ronald Cole received his Bachelor of Engineering in electrical engineering from University of New Haven. Ronald has more than 30 years of petrochemical, utility, and consulting experience. He is currently a supervisor of nuclear engineering electrical and instrumentation and controls at Dominion Energy's Millstone Nuclear Power Station. He is a member of the IEEE.

Richard Tuck received the BS degree in electrical engineering from Virginia Commonwealth University in 2012. He started his career working at one of Dominion Energy's nuclear generation facilities. He has spent the last four years with Dominion Energy, Richmond, VA, in the system protection engineering department where he has worked on distribution and transmission protection modeling and fault analysis.

Thomas Solinsky received his Bachelor of Engineering in electrical engineering from State University of New York, Maritime College, an MS degree in electrical engineering and an MS in management with a concentration in finance from Rensselaer Polytechnic Institute. Thomas has more than 30 years of utility and consulting experience. He is currently the manager of electrical and instrumentation and controls engineering for Zachry Nuclear Engineering. Also, he is a member of the IEEE, Nuclear Power Engineering Committee (NPEC), Auxiliary Power Subcommittee (SC-4).

Carolyn Sun received her BS degree in engineering from the University of British Columbia. She has five years of engineering consulting and utility experience in Canada. Since moving to the U.S. in 2019, Carolyn has worked at Schweitzer Engineering Laboratories, Inc. (SEL) engineering services where she has primarily executed studies using short-circuit and electromagnetic transient programs, performed hardware-in-the-loop testing, and developed relay settings. She is a member of the IEEE.

Ritwik Chowdhury received his BS degree in engineering from the University of British Columbia and his MS degree in engineering from the University of Toronto. He joined Schweitzer Engineering Laboratories, Inc. (SEL) in 2012, where he has worked as an application engineer and is presently a senior engineer in the research and development division. Ritwik holds 7 patents and has helped author 20 technical papers in the area of power system protection and point-on-wave controlled switching. He is the vice-chair of the Relaying Practices Subcommittee (I-SC) at the IEEE PSRC committee and the chair of two IEEE Standards Working Groups. He is a senior member of the IEEE and a registered professional engineer in the province of Ontario.

Ahmed Abd-Elkader received his Bachelor of Science in electrical engineering, with honors, from Ain Shams University, Cairo, Egypt, in 2008 and an MBA, with honors, from Wake Forest University, Winston-Salem, NC, in 2015. He is currently pursuing a PhD in electrical engineering from the University of North Carolina, He is a senior engineer with Schweitzer Engineering Laboratories, Inc. (SEL) with over 13 years' experience in power systems protection and control.

Bernard Matta received his BS degree in electrical engineering from Pennsylvania State University. He joined Virginia Power (presently Dominion Energy) in 1986 and worked in the system protection department calculating relay settings, performing system studies, testing protection systems, and writing standard procedures. He was on a team that evaluated and implemented microprocessor-based relays to replace electromechanical equipment. Bernard joined Schweitzer Engineering Laboratories, Inc. (SEL) in 2000. He has served many electric utilities and customers throughout the U.S. by providing relay settings to protect transmission, distribution, and generation equipment. Bernard is an IEEE member.